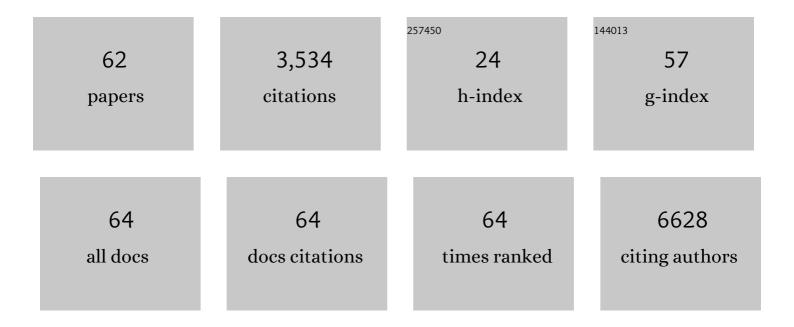
Eric Prestat

List of Publications by Year in descending order

Source: https://exaly.com/author-pdf/7822388/publications.pdf Version: 2024-02-01



FDIC DDESTAT

#	Article	IF	CITATIONS
1	Tunable sieving of ions using graphene oxide membranes. Nature Nanotechnology, 2017, 12, 546-550.	31.5	1,364
2	Quality Heterostructures from Two-Dimensional Crystals Unstable in Air by Their Assembly in Inert Atmosphere. Nano Letters, 2015, 15, 4914-4921.	9.1	358
3	Desalination and Nanofiltration through Functionalized Laminar MoS ₂ Membranes. ACS Nano, 2017, 11, 11082-11090.	14.6	275
4	Van der Waals pressure and its effect on trapped interlayer molecules. Nature Communications, 2016, 7, 12168.	12.8	137
5	A simple electrochemical route to metallic phase trilayer MoS ₂ : evaluation as electrocatalysts and supercapacitors. Journal of Materials Chemistry A, 2017, 5, 11316-11330.	10.3	119
6	Cation-controlled wetting properties of vermiculite membranes and its promise for fouling resistant oil–water separation. Nature Communications, 2020, 11, 1097.	12.8	89
7	Crossover from Spin Accumulation into Interface States to Spin Injection in the Germanium Conduction Band. Physical Review Letters, 2012, 109, 106603.	7.8	76
8	Electron Microscopy (Big and Small) Data Analysis With the Open Source Software Package HyperSpy. Microscopy and Microanalysis, 2017, 23, 214-215.	0.4	74
9	The Effects of Extensive Glomerular Filtration of Thin Graphene Oxide Sheets on Kidney Physiology. ACS Nano, 2016, 10, 10753-10767.	14.6	70
10	Real-time imaging and elemental mapping of AgAu nanoparticle transformations. Nanoscale, 2014, 6, 13598-13605.	5.6	64
11	Size Dependence of Exchange Bias in <mml:math <br="" xmlns:mml="http://www.w3.org/1998/Math/MathML">display="inline"><mml:mi>Co</mml:mi><mml:mo>/</mml:mo><mml:mi>CoO</mml:mi></mml:math> Nanostruct Physical Review Letters, 2012, 108, 077205.	u 768.	60
12	Enhanced organophilic separations with mixed matrix membranes of polymers of intrinsic microporosity and graphene-like fillers. Journal of Membrane Science, 2017, 526, 437-449.	8.2	57
13	Synergistic enhancement of gas selectivity in thin film composite membranes of PIM-1. Journal of Materials Chemistry A, 2019, 7, 6417-6430.	10.3	55
14	Observing Imperfection in Atomic Interfaces for van der Waals Heterostructures. Nano Letters, 2017, 17, 5222-5228.	9.1	53
15	Splenic Capture and <i>In Vivo</i> Intracellular Biodegradation of Biological-Grade Graphene Oxide Sheets. ACS Nano, 2020, 14, 10168-10186.	14.6	51
16	Self-catalytic membrane photo-reactor made of carbon nitride nanosheets. Journal of Materials Chemistry A, 2016, 4, 11666-11671.	10.3	47
17	Scalable Patterning of Encapsulated Black Phosphorus. Nano Letters, 2018, 18, 5373-5381.	9.1	43
18	Corrosion performance of Ti3SiC2, Ti3AlC2, Ti2AlC and Cr2AlC MAX phases in simulated primary water conditions. Corrosion Science, 2018, 139, 444-453.	6.6	41

Eric Prestat

#	Article	IF	CITATIONS
19	Study on the formation of thin film nanocomposite (TFN) membranes of polymers of intrinsic microporosity and graphene-like fillers: Effect of lateral flake size and chemical functionalization. Journal of Membrane Science, 2018, 565, 390-401.	8.2	38
20	The application of in situ analytical transmission electron microscopy to the study of preferential intergranular oxidation in Alloy 600. Ultramicroscopy, 2017, 176, 46-51.	1.9	37
21	Synthesis and characterization of composite membranes made of graphene and polymers of intrinsic microporosity. Carbon, 2016, 102, 357-366.	10.3	34
22	Self-Assembled 1T-MoS ₂ /Functionalized Graphene Composite Electrodes for Supercapacitor Devices. ACS Applied Energy Materials, 2022, 5, 61-70.	5.1	31
23	Electrical and thermal spin accumulation in germanium. Applied Physics Letters, 2012, 101, .	3.3	28
24	Role of 2D and 3D defects on the reduction of LaNiO3 nanoparticles for catalysis. Scientific Reports, 2017, 7, 10080.	3.3	27
25	Stable, concentrated, biocompatible, and defect-free graphene dispersions with positive charge. Nanoscale, 2020, 12, 12383-12394.	5.6	23
26	Interface-driven phase separation in multifunctional materials: The case of the ferromagnetic semiconductor GeMn. Physical Review B, 2012, 85, .	3.2	22
27	An in situ and ex situ TEM study into the oxidation of titanium (IV) sulphide. Npj 2D Materials and Applications, 2017, 1, .	7.9	21
28	Exploring Environmental Reactions in "Real World" Materials using In Situ Analytical TEM. Microscopy and Microanalysis, 2018, 24, 292-293.	0.4	21
29	Potential dependent ionic sieving through functionalized laminar MoS ₂ membranes. 2D Materials, 2020, 7, 015030.	4.4	21
30	Self-Limiting Growth of Two-Dimensional Palladium between Graphene Oxide Layers. Nano Letters, 2019, 19, 4678-4683.	9.1	18
31	Convergent beam electron holography for analysis of van der Waals heterostructures. Proceedings of the National Academy of Sciences of the United States of America, 2018, 115, 7473-7478.	7.1	17
32	Free, flexible and fast: Orientation mapping using the multi-core and GPU-accelerated template matching capabilities in the Python-based open source 4D-STEM analysis toolbox Pyxem. Ultramicroscopy, 2022, 237, 113517.	1.9	17
33	Electrically pumped WSe2-based light-emitting van der Waals heterostructures embedded in monolithic dielectric microcavities. 2D Materials, 2020, 7, 031006.	4.4	16
34	Enhanced Intraliposomal Metallic Nanoparticle Payload Capacity Using Microfluidic-Assisted Self-Assembly. Langmuir, 2019, 35, 13318-13331.	3.5	14
35	Composition and morphology of self-organized Mn-rich nanocolumns embedded in Ge: Correlation with the magnetic properties. Journal of Applied Physics, 2012, 112, .	2.5	13
36	Enhanced liquid phase exfoliation of graphene in water using an insoluble bis-pyrene stabiliser. Faraday Discussions, 2021, 227, 46-60.	3.2	12

Eric Prestat

#	Article	IF	CITATIONS
37	Coarsening of Pt nanoparticles on amorphous carbon film. Surface Science, 2013, 609, 195-202.	1.9	11
38	Mapping grain boundary heterogeneity at the nanoscale in a positive temperature coefficient of resistivity ceramic. APL Materials, 2017, 5, 066105.	5.1	11
39	Core-shell nanostructure in a <mml:math xmlns:mml="http://www.w3.org/1998/Math/MathML"><mml:mrow><mml:msub><mml:mi>Ge</mml:mi><mml:m observed via structural and magnetic measurements. Physical Review B, 2015, 91, .</mml:m </mml:msub></mml:mrow></mml:math 	11 342> < m i	ml: a :n>0.9∢
40	XEDS and EELS in the TEM at Atmospheric Pressure and High Temperature. Microscopy and Microanalysis, 2015, 21, 247-248.	0.4	8
41	Convergent and divergent beam electron holography and reconstruction of adsorbates on free-standing two-dimensional crystals. Frontiers of Physics, 2019, 14, 1.	5.0	7
42	Convergent beam electron diffraction of multilayer Van der Waals structures. Ultramicroscopy, 2020, 212, 112976.	1.9	6
43	lron-silica interaction during reduction of precipitated silica-promoted iron oxides using in situ XRD and TEM. Applied Catalysis A: General, 2021, 613, 118031.	4.3	6
44	Morphological and compositional changes of MFe2O4@Co3O4 (M = Ni, Zn) core-shell nanoparticles after mild reduction. Materials Characterization, 2019, 155, 109806.	4.4	5
45	Reply to: Random interstratification in hydrated graphene oxide membranes and implications for seawater desalination. Nature Nanotechnology, 2022, 17, 134-135.	31.5	5
46	Fate of Lu(III) sorbed on 2-line ferrihydrite at pHÂ5.7 and aged for 12Âyears at room temperature. II: insights from STEM-EDXS and DFT calculations. Environmental Science and Pollution Research, 2019, 26, 5282-5293.	5.3	4
47	Advanced semiconductor characterization with aberration corrected electron microscopes. Journal of Physics: Conference Series, 2013, 471, 012001.	0.4	3
48	Plasmon-induced nanoscale quantised conductance filaments. Scientific Reports, 2017, 7, 2878.	3.3	3
49	Long-range oriented graphene-like nanosheets with corrugated structure. Chemical Communications, 2018, 54, 13543-13546.	4.1	3
50	In situ Analytical TEM of Ilmenite Reduction in Hydrogen. Microscopy and Microanalysis, 2015, 21, 565-566.	0.4	2
51	Imaging the Hydrated Microbe-Metal Interface Using Nanoscale Spectrum Imaging. Particle and Particle Systems Characterization, 2016, 33, 833-841.	2.3	2
52	Holographic reconstruction of the interlayer distance of bilayer two-dimensional crystal samples from their convergent beam electron diffraction patterns. Ultramicroscopy, 2020, 219, 113020.	1.9	2
53	Structure and magnetism in strained Ge1â^' <i>x</i> â^' <i>y</i> Sn <i>x</i> Mn <i>y</i> films grown on Ge(001) by low temperature molecular beam epitaxy. Applied Physics Letters, 2013, 103, .	3.3	1
54	Investigations of segregation phenomena in highly strained Mn-doped Ge wetting layers and Ge quantum dots embedded in silicon. Applied Physics Letters, 2014, 104, 102409.	3.3	1

ERIC PRESTAT

#	Article	IF	CITATIONS
55	Cross sectional STEM imaging and analysis of multilayered two dimensional crystal heterostructure devices. Microscopy and Microanalysis, 2015, 21, 107-108.	0.4	1
56	Temperature Programmed Reduction of a PdCu Bimetallic Catalyst via Atmospheric Pressure in situ STEM-EDS and in situ X-Ray Adsorption Analysis. Microscopy and Microanalysis, 2016, 22, 214-215.	0.4	1
57	TEM Specimen Preparation Using a Low Energy Ion Beam for Nuclear Metallic Materials. Microscopy and Microanalysis, 2019, 25, 1608-1609.	0.4	1
58	Real Time Evolution of the Reduction of Ilmenite in H2: A Correlative In Situ and Ex Situ Study. Microscopy and Microanalysis, 2016, 22, 54-55.	0.4	0
59	Understanding 2D Crystal Vertical Heterostructures at the Atomic Scale Using Advanced Scanning Transmission Electron Microscopy. Microscopy and Microanalysis, 2017, 23, 1714-1715.	0.4	Ο
60	Correlative Microscopy: Elucidating the Mechanisms of SCC in Structural Alloys in PWR Environments. Microscopy and Microanalysis, 2020, 26, 168-170.	0.4	0
61	Application of Modern Scanning/Transmission Electron Microscope with Pixelated STEM Detector for Radiation Damage Study. Microscopy and Microanalysis, 2020, 26, 394-395.	0.4	Ο
62	Exploring Nanoscale Precursor Reactions in Alloy 600 in H2/N2–H2O Vapor Using In Situ Analytical Transmission Electron Microscopy. Minerals, Metals and Materials Series, 2018, , 399-407.	0.4	0